J. Physiol. (1982), **329**, *pp.* 485–507
With 14 *text-figures*
Printed in Great Britain

BLOCK AND ACTIVATION OF THE PACE-MAKER CHANNEL IN CALF PURKINJE FIBRES: EFFECTS OF POTASSIUM, CAESIUM AND RUBIDIUM

BY DARIO DIFRANCESCO

From the Istituto di Fisiologia Generale e Chimica Biologica, Sez. Elettrofisiologia, via Mangiagalli 32, 20133 Milano, Italy

(*Received 4 December 1981*)

SUMMARY

1. The effects of low concentrations of Cs^+ (0·01–3mM) on the fully activated I–V relation $\bar{i}_f(E)$ for the pace-maker current in calf Purkinje fibres have been investigated. The action of Cs^+ is two-fold: in the negative region of the I–V curve Cs^+ induces a channel blockade; on the other hand, at more positive potentials Cs^+ can produce the opposite effect, i.e. a current increase.

2. Cs^+-induced blockade is concentration- and voltage-dependent, as observed on other cation channels. Data in the far negative voltage range (about −150 to −50 mV) can be fitted by a simple block model (Woodhull, 1973), which gives a mean value of 0·71 for the fraction of membrane thickness (δ) crossed by Cs^+ ions before reaching the blocking site. The value of δ does not appear to be affected by either external Na or external K concentrations. Values for the dissociation constant of the blocking reaction at $E = 0$ mV (k_0) are found in the range 0·5–3·7 mM. In the positive region of the $\bar{i}_f(E)$ relation the current depression caused by channel blockade vanishes. Unexpectedly, in this range the current can be observed to increase with Cs^+, and $\bar{i}_f(E)$ curves in different Cs^+ concentrations show cross-over.

3. Changing external K^+ also produces similar cross-over phenomena. Investigation of this effect reveals that the increase in slope of the I–V curve on raising the external K^+ concentration follows Michaelis–Menten kinetics, and can be interpreted in terms of K^+-induced channel activation. It is found that 44 ± 6 mM-K^+ half-saturates the channel activating reaction.

4. The Cs^+-induced current increase is large in low-K^+ solutions and vanishes in high-K^+ solutions, suggesting a competition between Cs^+ and K^+ ions in their activating action. Increasing Na^+ also limits the Cs^+-induced current increase.

5. Rb^+ also blocks the i_f channel, though less efficiently than Cs^+. The block caused by Rb^+ is, unlike that of Cs^+, nearly voltage-independent, and is explained by assuming that the blocking reaction occurs near the external mouth of the channel (mean value of δ is 0·05). The zero-voltage dissociation constant (k_0) of the Rb^+-blocking reaction ranges between 1·4 and 5·4 mM, and is lower in low-Na^+, high-K^+ solutions.

6. A possible characterization of the i_f channel which explains these results includes an inner 'blocking' site, to which external Cs^+ ions bind, blocking the

channel, and a more external 'activatory' site, to which K^+, Cs^+, Rb^+ and possibly Na^+ ions bind. Binding of K^+ to this site induces a current increase either by modulating the channel, or actually by opening the channel itself. A similar mechanism can apply to Cs^+ and to Rb^+ binding.

INTRODUCTION

The study of the concentration- and voltage-dependence of ionic blockade of a membrane channel is a first step in the characterization of the properties of the channel itself and provides part of the information required for channel modelling (Hille, 1975; Sandblom, Eisenman & Neher, 1977; Adelman & French, 1978; Ciani, Krasne & Hagiwara, 1980). Several K^+- or Na^+-selective channels from different tissues are known to be blocked by monovalent cations such as H^+, Cs^+, Rb^+ and Tl^+, or by divalent cations such such as Ba^{2+} and Sr^{2+} (Sperelakis, Schneider & Harris, 1967; Bezanilla & Armstrong, 1972; Hagiwara, Miyazaki & Rosenthal, 1976; Dubois & Bergman, 1977; Hagiwara, Miyazaki, Moody & Patlak, 1978; Gay & Stanfield, 1977; Standen & Stanfield, 1978*a*, *b*). The pace-maker current i_f is carried, according to its new interpretation, by both K^+ and Na^+ ions, and is known to be strongly depressed in the pace-maker range of voltages by Cs^+ in low concentrations (DiFrancesco, 1981*a*; Brown, DiFrancesco, Kimura & Noble, 1981), which suggests a Cs^+-induced channel blockade. This work started as an attempt to describe in more detail the blocking action of Cs^+ and of other potential blockers such as Rb^+, on the i_f channel in Purkinje fibres. The results show that even for a channel of low ionic selectivity such as the pace-maker channel, the current reduction due to Cs^+, and to a lesser extent Rb^+, is attributable to channel blockade.

Together with a blocking action both ions, but especially Cs^+, were found to exert an additional, stimulatory effect revealed by a current increase occurring on increasing the external Cs^+ (or Rb^+) concentration at positive potentials. The similarity of this 'activatory' action to the one exerted by K^+ on the same channel (DiFrancesco, 1981*b*) has prompted experiments aimed to give a qualitative description of this action, and to establish possible correlations between the activating actions of different cations on the pace-maker channel. Part of the results here reported have been published in abstract form (DiFrancesco, 1981*c*).

METHODS

Hearts freshly removed from calves were taken to the laboratory in cold (4 °C) heparinized cardioplegic solution containing (in mM): NaCl, 140; KCl, 20; $CaCl_2$, 1·8; $MgCl_2$, 16; $NaHCO_3$, 12; NaH_2PO_4, 0·4; procaine, 1·2; D-glucose, 1 g/l., and buffered to pH = 7·4 by bubbling with a 95% O_2 + 5% CO_2 mixture. Strands of fine Purkinje fibres were dissected and stored in oxygenated Tyrode solution at room temperature. Single fibres of length ranging from 4 to 7 mm and inner diameter of about 0·4 mm were fixed to the bottom of the perfusing chamber by means of a grid made of fine parallel stainless-steel pins at a distance of 1·8 mm from each other. The grid was laid on the fibre and then fixed to the chamber by screws. Progressive tightening of the grid on the fibre eventually resulted in electrical disconnexion between different segments without physically disrupting all the connective tissue beneath the pins. This method of securing the fibres has the advantage of fixing the length of the segment under study and of providing stable micro-electrode penetrations. Temperature in the perfusing chamber was kept constant at 35 ± 0·2 °C. The usual

methods and apparatus for voltage clamping the fibres were used (see for example DiFrancesco, 1981*a*). Bevelled 2–5 MΩ, 3 M-KCl and 5–8 MΩ, 3 M-K citrate micro-electrodes were used for voltage recording and current feeding, respectively. The fibres were allowed to recover in normal Tyrode for a variable period before passing a given control solution. Normal Tyrode solution was composed as follows (concentrations in mM): NaCl, 140; KCl, 3; $CaCl_2$, 1·8; $MgCl_2$, 1; $NaHCO_3$, 12; NaH_2PO_4, 0·4; D-glucose 1 g/l. and was continuously bubbled with 95% O_2 + 5% CO_2 to pH = 7·4. All other solutions were buffered with Tris HCl to pH = 7·4 and bubbled with O_2, and contained 5 mM-$MnCl_2$ and 5 mM-$BaCl_2$ used routinely to reduce the interference from slow-inward current transients and K^+-accumulation/depletion processes due to the time-independent current i_{K1} (see DiFrancesco, 1981*a*). The use of Mn^{2+} is also suggested by the recently published evidence that in calves' Purkinje fibres Mn^{2+} reduces the transient outward current i_{to} (Siegelbaum & Tsien, 1980), whose activation during depolarizations above 0mV could overlap i_f transients. The range where the $\bar{i}_f(E)$ relations can thus be investigated without significant contamination from other components is relatively large, extending from about −170/−180 mV to about +20 mV (see Figs. 2, 6, 9, 10 and 14). When needed, the Na^+concentration was reduced by substitution of NaCl with equimolar quantities of Tris HCl or, as specified by choline Cl. No difference was found between experimental results using either of these substitutes. The K^+ concentration was increased by adding KCl. When high K^+ concentrations were required (see for example Fig. 7) a low-Na^+ control solution was used throughout the experiment, and high K^+ concentrations were obtained by replacing the Na^+ substitute by K^+. The protocol of a typical experiment consisted of measuring the $\bar{i}_f(E)$ relation in a given control solution, and then in the same solution containing different concentrations of Cs^+ of Rb^+. The same procedure was then repeated for a set of different control solutions, where either the Na^+ or the K^+ concentration was varied. The method used to measure the $\bar{i}_f(E)$ relation was the same as described in DiFrancesco (1981*b*). Different series of blocking ion concentrations, allowing 2- to 5-fold increments, were used. Data analysis was performed on a desk HP-85 computer, which also a provided the graphical outputs shown in some of the figures.

RESULTS

Voltage-dependent blockade of the pace-maker channel induced by low concentrations of Cs^+

An example of current records illustrating the Cs^+-induced reduction of the current i_f is shown in Fig. 1. Envelope tests have been performed in a control solution, and in the same solution containing different Cs^+ concentrations, by applying from a holding potential of −27 mV hyperpolarizing pulses of various durations to −107 mV, followed by depolarizations to 3 mV. At this potential the current is outward in the 18 mM-K^+, 14 mM-Na^+ Tyrode solution, and therefore the de-activation of i_f results in an outward decaying tail. Perfusion with 0·07 mM-Cs^+ reduces the current activated during the negative pulse, but leaves almost unaltered the tail recorded during the following depolarization. With 0·7 mM-Cs^+ the current depression at −107 mV is even more pronounced, while still no reduction is seen at 3 mV. As expected (see DiFrancesco, 1981*b*), the time constants of current onset and tails envelope in Fig. 1*A* and *B* have similar values. It can be noticed that the current activation at −107 mV, as well as the tails envelope onset at +3 mV, are accelerated by Cs^+ (time constant of tails envelope varies from 277 msec in the control solution to 243 msec in 0·07 mM-Cs^+ and to 191 msec in 0·7 mM-Cs^+). Details of the effects of Cs^+ on the i_f kinetics have not been studied here, but acceleration of the time course of activation in Cs^+- and Rb^+-containing solutions has been often observed with envelope test method ($n = 6$). It is possible that the interactions described below of Cs^+ (and Rb^+) ions with the i_f channel have also a modulatory action on the current kinetics.

A fuller description of the voltage- and concentration-dependence of the Cs^+ action is given by plotting, as done in Fig. 2, the fully-activated $I-V$ relation in the control solution and after addition of the blocking ion. In the negative voltage region of the $I-V$ curve the block is characterized by a current depression which increases with the membrane polarization. This type of voltage-dependent blockade is similar to that exerted by Cs^+ on several other channels permeable to K^+ (Hagiwara *et al.*, 1976; Dubois & Bergman, 1977; Gay & Stanfield, 1977; Adelman & French, 1978; Coronado

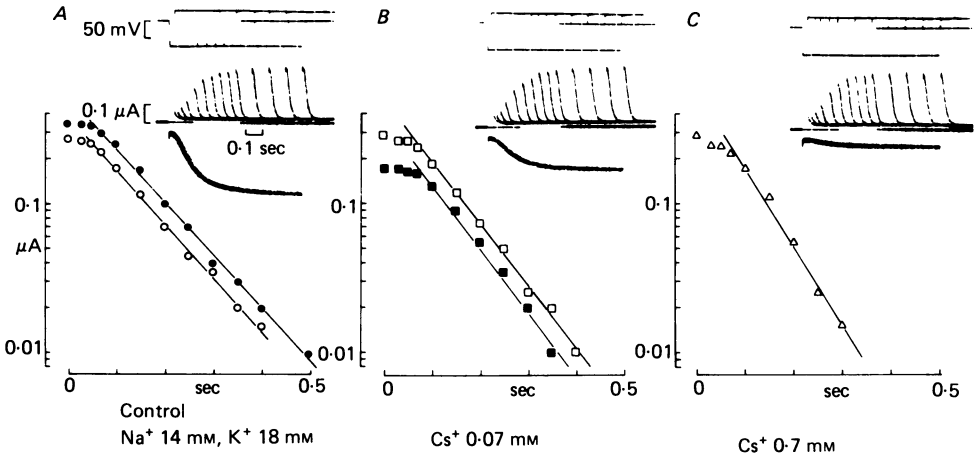

Fig. 1. Envelope tests in a control solution containing K^+, 18 mM and Na^+, 14 mM (*A*) and in the same solution after addition of Cs^+ 0·07 (*B*) and 0·7 mM (*C*). Na^+ substituted by choline. Graded i_f activation was obtained by hyperpolarizing to −107 mV for variable durations. Outward decaying tails reflecting i_f de-activation were then recorded at +3 mV. Semilogarithmic plots of the amplitudes of onsetting currents (filled symbols) and decaying tails (open symbols) against the negative pulse duration are shown below the current records. Time constants of least-squares fitting lines (calculated from 50 msec on) are, from left to right (in msec): 277 (○), 282 (●), 236 (■), 243 (□) and 191 (△). Current activated in *C* was too small to be reliably measured.

& Miller, 1979; Carmeliet, 1979). From the experiments of Fig. 2, however, it also appears that the action of Cs^+ is not simply that of blocking the channel. Indeed, in the far positive range of the $I-V$ curve, the current in the presence of Cs^+ tends to become *larger* than that in the control solution. This is particularly evident in the experiment shown in Fig. 2*B*, where Cs^+ in the concentration of 0·5 mM was added to a 6 mM-K^+, 14 mM-Na^+ solution. This aspect of the action of Cs^+ is dealt with below, where experiments are described showing how Cs^+, and to a lesser extent Rb^+, behave like activating ions, and how this effect is linked to the activating action of K^+.

Position of the Cs^+ blocking site

According to the single-ion channel model of Woodhull (1973), the phenomenon of progressive reduction of the current with negative membrane potential seen in Fig. 2 can be explained by assuming that the blocking ion enters the channel and runs a fraction of the membrane thickness before blocking the channel itself. According the this interpretation the block increases at more negative voltages because of the augmented probability that the inner site is occupied by the blocking ion. The presence of the activation-like effect of Cs^+ on the i_f channel noted above puts,

however, some limits to a quantitative analysis of its blocking effect. In practice, the blocking action can be considered as the predominant one in only the far negative region of the $\bar{i}_f(E)$ curve, because only in this range will the probability that the ion interaction with the channel is of the blocking type, as induced by Cs^+ binding to an inner site, become substantially larger than that of any other interaction occurring at a more external site.

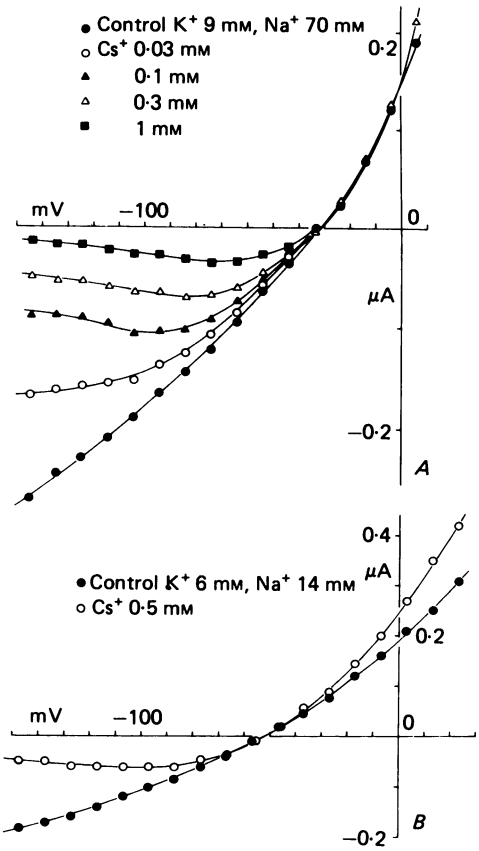

Fig. 2. *A*, $\bar{i}_f(E)$ relations in 9 mM-K^+, 70 mM-Na^+ control solution and after addition of 0·03–1 mM-Cs^+. *B*, same in a 6 mM-K^+, 14 mM-Na^+ control solution and after addition of 0·5 mM-Cs^+. Here the Cs^+-induced current increase in the positive range of the curve is particularly evident. Na^+ substituted by Tris in *A* and by choline in *B*.

Fig. 3 shows semilog plots of the ratio $r = I_{Cs}/(I-I_{Cs})$ (which will be referred to below as the relative blocking ratio) as a function of membrane potential, for an experiment where Cs^+ in concentrations ranging from 0·03 to 1 mM was added to solutions containing different concentrations of K^+ and Na^+. According to Woolhull's block model, on the simplifying assumption that Cs^+ ions can only enter the channel from outside, the relative blocking ratio can be related to the Cs^+ concentration and the membrane potential by the following equation (see Discussion for its derivation)

$$\ln r = \ln\left(I_{Cs}/(I-I_{Cs})\right) = \delta\frac{E}{RT/F} - \ln\left([Cs]/k_0\right), \qquad (1)$$

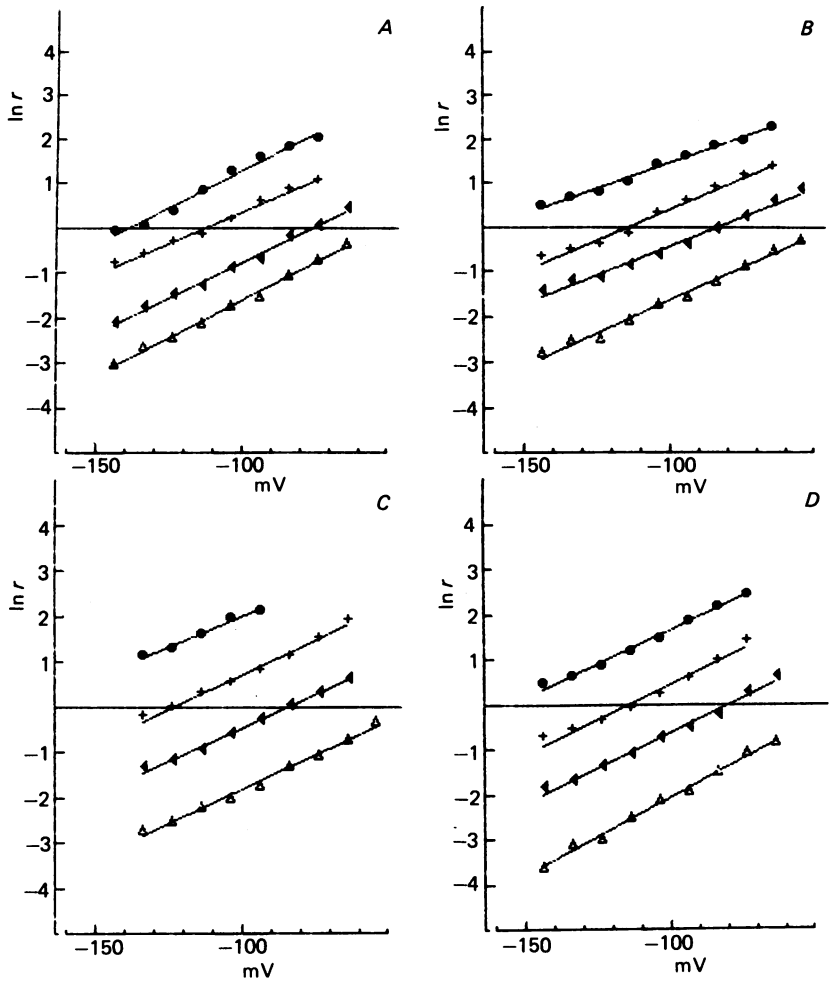

Fig. 3. Voltage-dependence of Cs^+ block in an experiment where 0·03 (○), 0·1 (+), 0·3 (◀) and 1 (△) mM-Cs^+ were added to four different solutions containing K^+ and Na^+ in the following concentrations (in mM) respectively: 9, 14 (*A*), 9, 70 (*B*), 18, 70 (*C*) and 18, 14 (*D*). Natural logarithm of the relative blocking ratio $r\,(=I_{Cs}/(I-I_{Cs}))$ is plotted against membrane potential for each Cs^+ concentration. Values of I and I_{Cs} refer to fully activated $\bar{i}_f(E)$ values in control and in presence of Cs^+ respectively, measured at the same potential from *I–V* relations like those shown in Fig. 2. For each curve an upper voltage limit is selected such that the difference between I and I_{Cs} is not too small, to avoid large scattering in the ratio r. Values of δ calculated using eqn. (1) from the slopes of least-squares fitting lines are (top to bottom): 0·818, 0·690, 0·788, 0·819 (*A*), 0·568, 0·686, 0·646, 0·721 (*B*), 0·671, 0·753, 0·729, 0·750 (*C*) and 0·735, 0·764, 0·779, 0·867 (*D*). Mean δ in this experiment is $0·736 \pm 0·07$.

where δ is the fraction of membrane thickness crossed by Cs^+ ions before reaching the blocking site ('electrical' distance), and k_0 is the dissociation constant of the binding reaction at $E = 0$ mV. Eqn. (1) is valid on condition that other ions do not interfere with Cs^+ binding and that the current carried by Cs^+ is negligible. The results of Fig. 3 show that $\ln r$ and E are linearly related in at least the far negative range

of the $I-V$ relation, and that apart from random experimental scattering the slope of the least-squares fitting lines does not substantially depend on either the Cs^+ or the Na^+ and K^+ concentrations. This is confirmed by the results shown in Table 1, where values of the slopes from $n = 102$ similar curves (eleven experiments) in different ionic conditions are reported. From these values an average $\delta = 0{\cdot}71 \pm 0{\cdot}13$ can be calculated.

TABLE 1. Values of δ relative to Cs^+ block calculated according to eqn. (1) from eleven experiments at various K^+ and Na^+ concentrations (shown in mM)

	$[K^+]$(mM) 6	9	18	24	36
$[Na^+]$	*c* 0·678 ± 0·10 (2)	*a* 0·820 ± 0·02 (2)	*a* 0·587 ± 0·11 (3)	*d* 0·765 ± 0·07 (3)	*b* 0·770 ± 0·05 (3)
(mM)	*e* 0·782 (1)	*b* 0·812 ± 0·02 (2)	*b* 0·626 ± 0·06 (3)	—	*f* 0·648 ± 0·13 (2)
14	*l* 0·581 ± 0·16 (5)	*m* 0·779 ± 0·06 (4)	*e* 0·738 ± 0·07 (2)	—	*g* 0·816 (1)
	—	—	*l* 0·809 ± 0·10 (5)	—	*l* 0·846 ± 0·13 (5)
	—	—	*m* 0·786 ± 0·06 (4)	—	—
35	*i* 0·681 ± 0·08 (2)	*h* 0·639 ± 0·10 (5)	*i* 0·678 ± 0·18 (4)	*h* 0·789 ± 0·06 (5)	*i* 0·673 ± 0·26 (5)
70	*c* 0·742 ± 0·09 (3)	*m* 0·655 ± 0·06 (4)	*m* 0·726 ± 0·04 (4)	*d* 0·692 ± 0·12 (3)	*f* 0·711 ± 0·04 (2)
140	*c* 0·733 ± 0·01 (3)	*h* 0·648 ± 0·08 (5)	*e* 0·531 ± 0·15 (2)	*h* 0·618 ± 0·05 (5)	*f* 0·674 ± 0·06 (2)

The method for obtaining the reported values is the same as described in Fig. 3. Letters *a–m* refer to different experiments. Each δ value is expressed as mean ± S.D. and is followed by the number of averaged points within parentheses.

Dependence of block on the Cs^+ concentration

The concentration dependence of the block induced by Cs^+ can be characterized by plotting, as done in Fig. 4, the relative blocking ratio $r = I_{Cs}/(I - I_{Cs})$ against the reciprocal of Cs^+ concentration for several membrane potentials. The plots are from an experiment where Cs^+ concentration was changed in the range 0·03–3 mM in four different solutions and show that, again in the far negative voltage range, a linear relation is observed as predicted by the blocking model outlined above. The slope of each least-squares fitting line in Fig. 4 represents the dissociation constant $k(E)$ of the binding reaction at the corresponding voltage. Plotting these values on a semilog scale against membrane potential in Fig. 5 yields, as expected from the results described in the previous section, roughly linear relations, indicating that for all four cases the dependence of the dissociation constant on membrane potential can be approximated by a simple exponential function. The values of the dissociation constants at zero membrane potential (k_0) as deduced from the data of Fig. 4 by extrapolation to $E = 0$ mV are (in mM): 2·49 (*A*), 1·54 (*B*), 1·70 (*C*) and 1·85 (*D*). In Table 2 similar results from $n = 5$ experiments are reported. From these data neither K^+ nor Na^+ seems to have an appreciable effect on the value of k_0. However, it must be noted that, given the way the k_0 values are obtained (i.e. by extrapolation to $E = 0$ from data in a limited voltage range), they are likely to be subjected to a large scattering. Thus, small effects of changing external Na^+ and K^+ concentrations on the zero-voltage dissociation constant cannot be appreciated. To have a more reliable indication of possible effects of K^+ and Na^+ on Cs^+ binding, extrapolated values of the dissociation constant $k(-100)$ at $E = -100$ mV, where the error introduced by

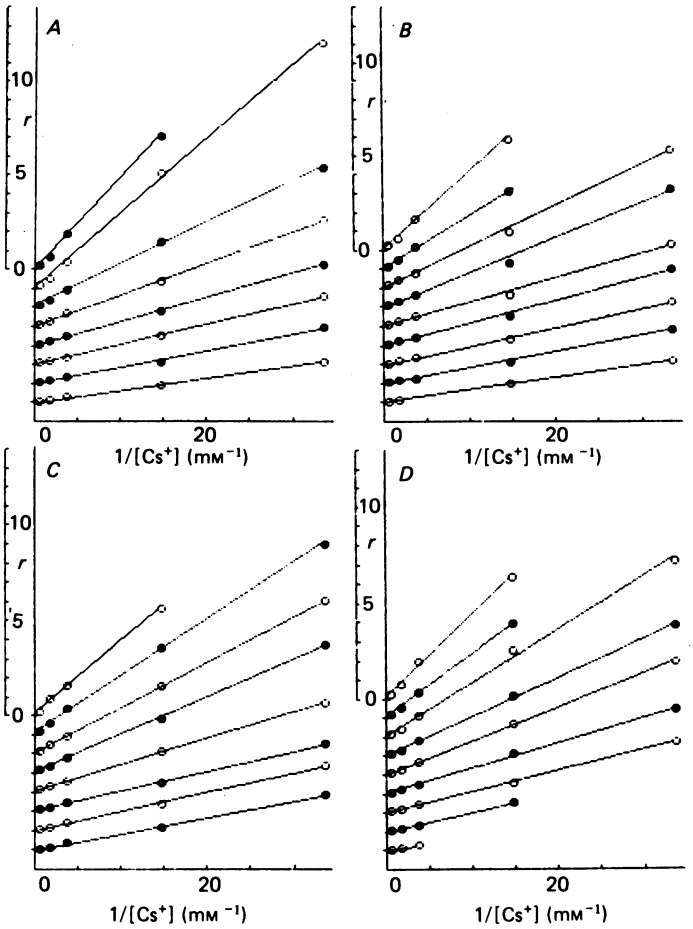

Fig. 4. Concentration-dependence of Cs^+ block in an experiment analogous to that shown in Fig. 3. Control solutions contained K^+ and Na^+ in the following concentrations (in mM): 24, 35 (*A*), 9, 35 (*B*), 9, 140 (*C*) and 24, 140 (*D*). Na^+ substituted by Tris. Cs^+ concentrations used were 0·03, 0·07, 0·3, 0·7 and 3 mM. The relative blocking ratio *r*, measured as described in Fig. 2, is plotted for different membrane potentials against the reciprocal of Cs^+ concentration. In each panel, curves are shifted vertically by fixed arbitary amounts for clarity, and are marked with alternatively open and filled circles. From top to bottom in all panels, each curve corresponds to a membrane potential increasing in 10 mV negative steps, and starting from: −56 (*A*) −66 mV (*B*, *C* and *D*).

scattering of the fitting parameters is less than that at $E = 0$ mV, are also reported in Table 2. Again, no clear cut effect of either Na^+ or K^+ on Cs^+ binding appears from these data. A substantial increase of $k(-100)$ is indeed apparent in two out of five experiments on increasing the external Na^+ concentration (*d* at 18 mM-K^+ and *a* at 24 mM-K^+), but in the remaining three cases (*a* and *d* at 9 mM-K^+ and *b* at 36 mM-K^+) $k(-100)$ changes only slightly. An even more irregular behaviour is observed on changing the external K^+ concentration.

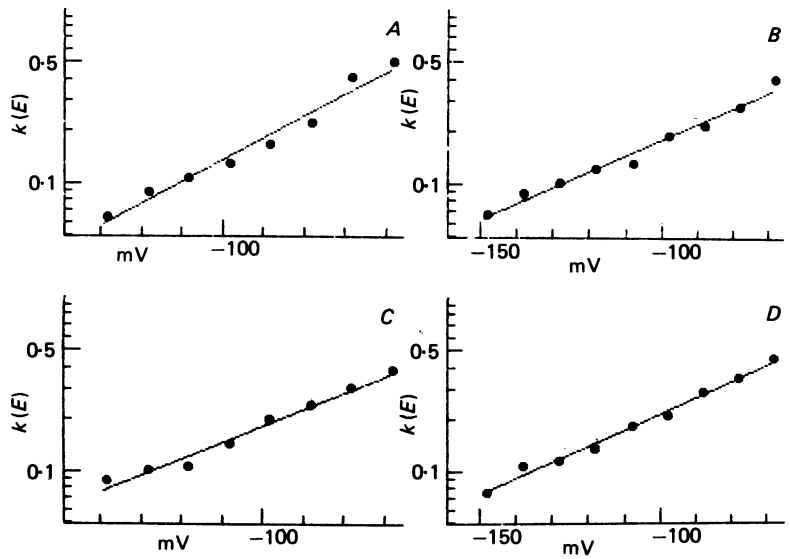

Fig. 5. Voltage-dependence of the dissociation constant $k(E)$ for Cs^+ block. Slopes of best-fitting lines from the data in Fig. 4 are plotted against membrane potential on semilog scale (panels *A–D* correspond to the same external K^+ and Na^+ concentrations as panels *A –D* in Fig. 4, respectively). The plots indicate that $k(E)$ can be approximated by an exponential function (see eqn. (6*b*) of Discussion). Extrapolation of the least-squares fitting lines to $E = 0$ mV gives the following values for the zero-voltage dissociation constant k_0 (*A–D*, values in mM): 2·49, 1·54, 1·70 and 1·85. Mean k_0 in this experiment is $1·90 \pm 0·42$.

TABLE 2. Values of zero-voltage dissociation constant (k_0) and of the dissociation constant at $E = -100$ mV ($k(-100)$) for the Cs^+ block, reported from five experiments (*a–e*) at various K^+ and Na^+ concentrations

	[K^+](mM) 6	9	18	24	36
[Na^+] 14		*d* 2·81	*d* 2·90		*b* 2·69
(mM)		0·103	0·155		0·298
	e 0·51		*e* 3·72		*e* 2·42
	0·092		0·250		0·189
35	*c* 2·23	*a* 1·54	*c* 1·60	*a* 2·49	*c* 1·02
	0·140	0·181	0·118	0·136	0·104
70		*d* 1·11	*d* 3·63		
		0·121	0·226		
140		*a* 1·70		*a* 1·85	*b* 2·88
		0·184		0·214	0·288

The values were obtained by extrapolation to $E = 0$ mV and to $E = -100$ mV of the $k(E)$ plots as shown in Fig. 5. For each experiment the upper value is k_0 and the lower one $k(-100)$.

K^+-induced activating action on the i_f channel

As noted in Fig. 2 above, in the positive voltage range of the $\bar{i}_f(E)$ relation a tendency of the current to increase is observed after exposure to Cs^+. A similar tendency has also been observed when external K^+ is changed (DiFrancesco, 1981*b*). Crossing-over of *I–V* curves in different K^+ concentrations can be attributed, as for

the K^+-inward rectifier in the skeletal muscle (Armstrong, 1969; Hille & Schwarz, 1978; Standen & Stanfield, 1978*b*) to a voltage- and concentration-dependent block caused by an internal ion. The intersection of two *I–V* curves is in this case the secondary effect of the presence of a region where the slope conductance is negative. Thus, a similar interpretation cannot be applied to the pace-maker channel case, as

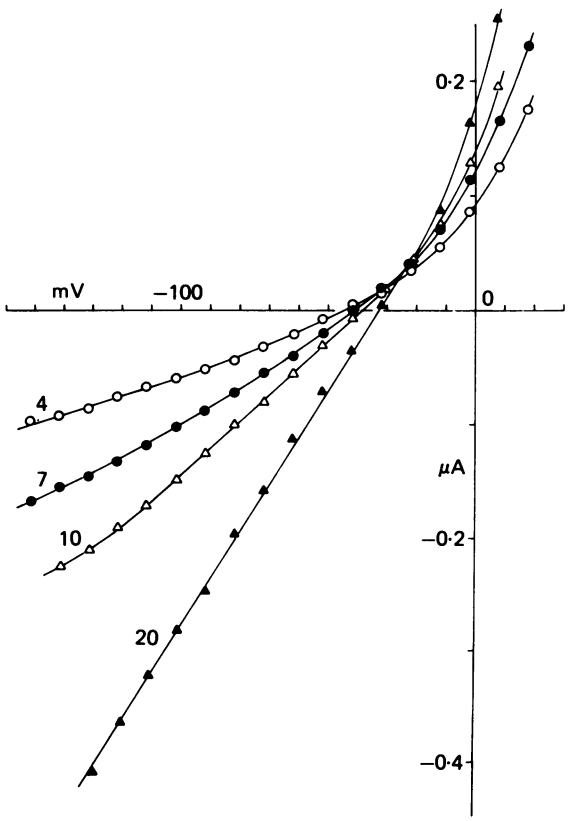

Fig. 6. $\bar{i}_f$ (E) relations in different K^+ concentrations (indicated in mM by each curve). The Na^+ concentration was 35 mM throughout (choline used as a substitute). Curves in 5 and 40 mM-K^+, also measured in the same experiment, have been omitted for clarity.

here the crossing-over occurs at voltages where the $\bar{i}_f(E)$ relation has a positive slope (see Fig. 6). A more likely interpretation of the cross-over phenomenon observed in different K^+ concentrations is that K^+ ions have an activating action on the i_f channel. This is suggested by the evidence that the current i_f, normally carried by both K^+ and Na^+ ions, tends to disappear on lowering the external K^+ concentration, even when the Na^+ gradient is not zero (see Fig. 8). Such an action would also provide a straightforward interpretation of the increase in total slope conductance caused by increasing external K^+, as shown in Fig. 6. Examples of K^+-induced K-channel activation have been already described (for example, Dubois & Bergman, 1977; Standen & Stanfield, 1978*b*). Given that K^+ carries part of the current, a suitable indication of a possible activating mechanism induced by external K^+ ions on the

i_f channel is given by studying the dependence of the channel slope conductance on the K^+ concentration. Fig. 7 shows results from $n = 8$ experiments where the fully-activated $I-V$ relation was measured in different K^+ concentrations. In each experiment, a limited voltage range can be selected in the central region of the $I-V$ relations where all curves are approximately linear, and where serious distortions

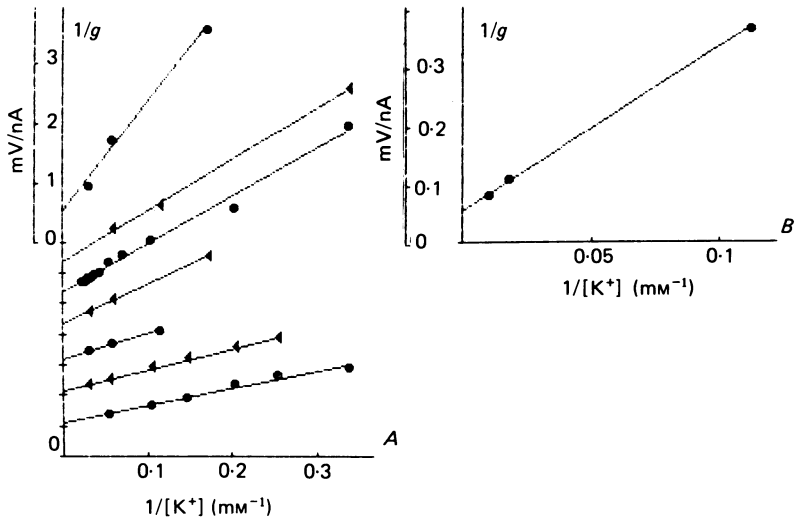

Fig. 7. Double-reciprocal plots for the dependence of total currrent slope conductance on K^+ concentration. *A*, results from seven different experiments where $I-V$ relations were measured in several K^+ concentrations, ranging from 3 to 40 mM. In each experiment a fixed voltage range was selected and slopes of the $i_f(E)$ relations in different K^+ concentrations were calculated from linear best-fitting to experimental points (for fuller explanation see text). The slope reciprocal, in mV/nA, is then plotted against reciprocal of K^+ concentration (in mM^{-1}). Curves are shifted vertically for clarity and have been arbitrarily ordered according to their slope. By use of eqn. (2), from slope and intercept to $1/[K] = 0$ of the best-fitting lines, values of the equilibrium constant k_K for the K^+-activating reaction (reaction (7) in the Discussion) can be calculated. From top to bottom these are (in mM): 34·7, 46·5, 39·8, 40·6, 45·8, 44·5 and 50·1. *B*, a similar plot referring to an experiment where high K^+ concentrations (up to 108 mM) were used, and giving a k_K value of 51·5 mM. Note reduced scales in comparison with *A*. From top to bottom, *A* to *B*, Na^+ concentrations (in mM) and Na-substitutes were: 35 (Tris), 35 (choline), 140, 14 (choline), 14 (Tris), 35 (choline), 70 (Tris), 35 (Tris).

from residual accumulation/depletion phenomena are unlikely to occur. For example, in the experiment of Fig. 6, also reported in Fig. 7, the voltage range selected for linear least-squares fitting was -105 to -35 mV. The slope of each fitting line in this range represents the total channel slope conductance at each K^+ concentration.

Here it is assumed that $i_f(E)$ can be described as the product $i_f(E) = \bar{g}_f \cdot (E - E_f)$, $\bar{g}_f$ being the total channel conductance and E_f the reversal potential. This assumption is valid if, as done in Fig. 6, a limited voltage range is considered, but the presence of outward-going rectification, particularly in the far positive region of the $I-V$ curve (see for example also Figs. 2, 9 and 14) clearly indicates that it can only be considered as a first approximation. As discussed below, however (see Discussion), the above assumption is not strictly necessary in the analysis of the activating action induced by K^+, and the results reported below are independent from it.

Fig. 7 shows that the reciprocal of $\bar{g}_f$ measured as indicated is linearly related to the reciprocal of K^+ concentration, as expected for a simple Michaelis–Menten activation mechanism. From the data in Fig. 7 values of the dissociation constant k_K for the activating reaction, as derived using the equation:

$$\bar{g}_f = \bar{g}_{fM} \cdot \frac{[K]}{[K]+k_K}, \tag{2}$$

can be calculated. The large variability in the slope of the $1/g$ *versus* $1/[K]$ functions in Fig. 7 depends on the total amount of current passing through the preparation, and thus ultimately on the fibre's size. The k_K values obtained are all in the same range (34·7, 46·4, 39·8, 40·6, 45·8, 44·5 and 50·1 mM, respectively from top to bottom curve in Fig. 7*A*). Fig. 7*B* shows an experiment where, in order to obtain a more reliable indication of the saturation value of the maximal conductance ($\bar{g}_{fM}$), the high-K^+ concentration range was investigated (up to 108 mM-K^+). The value for k_K obtained in this experiment was 51·5 mM. The mean value of k_K from all the data in Fig. 7 is 44·2 ± 5·6 mM. No obvious depencence on the external Na^+ concentration, varied in the range 14–140 mM, appears from these data.

Cs^+-induced current augmentation at different external K^+ concentrations

The Cs^+-induced increase of $\bar{i}_f$ observed in the positive voltage range (Fig.2) cannot be analysed with the same degree of accuracy as that induced by K^+, because of overlap of the blocking effects of Cs^+. Information on the mode of action of Cs^+ in inducing the observed current increase can nevertheless be obtained, for example by investigating possible interactions between Cs^+ and K^+ in their activating actions. Fig. 8 shows an experiment where *I–V* curves in different Cs^+ concentrations are recorded in a K^+-free solution. It is interesting to observe that while no current can be detected negative to about −50 mV, in K^+-free solutions a substantial amount of i_f (about ½ of that in 3 mM-K^+ solution in this case) can be recorded positive to this range. The presence of some current in this range is not in contrast with the hypothesis that external K^+ activates the channel: on the contrary, it is what would be expected if some potassium, due to accumulation phenomena, is present in the intercellular spaces (clefts) even during perfusion with a K^+-free solution. The absence of a measurable i_f component in the voltage range negative to −60 mV could be attributed in this case to the removal of this residual K^+-induced activation by depletion of cleft K^+ taking place during hyperpolarizations. Fig. 8 shows that 0·5 mM-Cs^+ greatly increases the current recorded positive to −50 mV. Since Cs^+ ions, being present only in the external solution, can hardly contribute any current in the outward direction, the Cs^+-induced current increase is more probably the effect of an interaction of Cs^+ with the i_f channel.

If the current increase in Cs^+ is of the same nature of that seen on increasing K^+, i.e. is due to an activating action, it is possible to check whether the two ions interact with each other in their action. This is done in the experiment shown in Fig. 9, where the effects of various Cs^+ concentrations are followed in solutions containing different amounts of K^+. It appears that the current increase induced by Cs^+ is very large at low K^+, but it vanishes at high K^+ concentrations. This is expected if both ions act

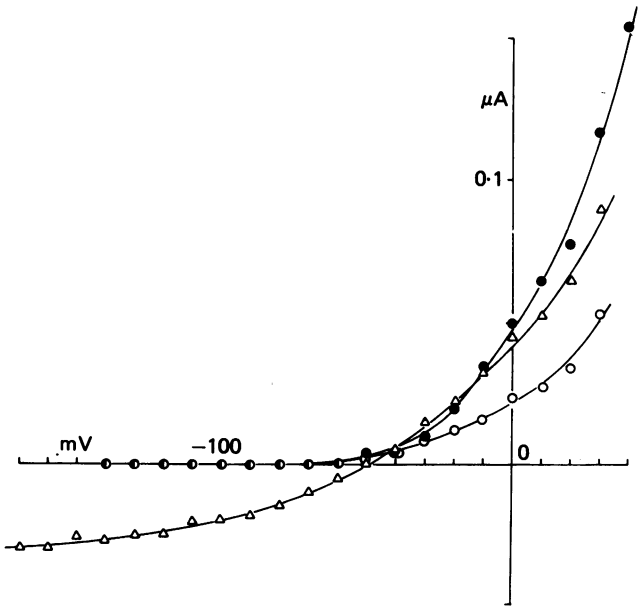

Fig. 8. $\bar{\imath}_f(E)$ relations measured in a control solution containing 3mM-K^+ (△), in a K^+-free solution (○) and in a K^+-free solution after addition of Cs^+ 0·5 mM (●). Na^+ concentration was 35 mM throughout (choline used as substitute).

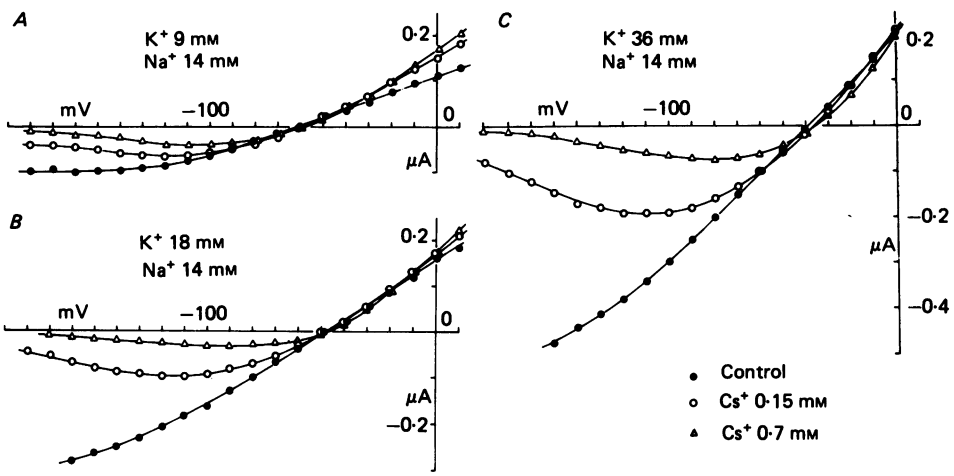

Fig. 9. $\bar{\imath}_f(E)$ relations measured in three control solutions containing different K^+ concentrations, and after addition of 0·15 and 0·7 mM-Cs^+, as indicated in each panel. Notice how the increase in external K^+ concentration reduces the extent by which Cs^+ increases the current in the outward direction in the range near 0 mV. Na substituted by Tris.

at the same activating site in a competitive way. The effect shown in Fig. 9 has been observed qualitatively in $n = 6$ experiments where the K^+ concentration was changed in the range 6–36 mM, and is also present to a lesser extent when the Na^+ concentration is changed at a fixed K^+ ($n = 3$ experiments, not shown). These results agree with the idea that the pace-maker channel possesses an activating site to which Cs^+, K^+ and Na^+ bind competitively, and that the binding of K^+ and Cs^+ triggers the channel activating process.

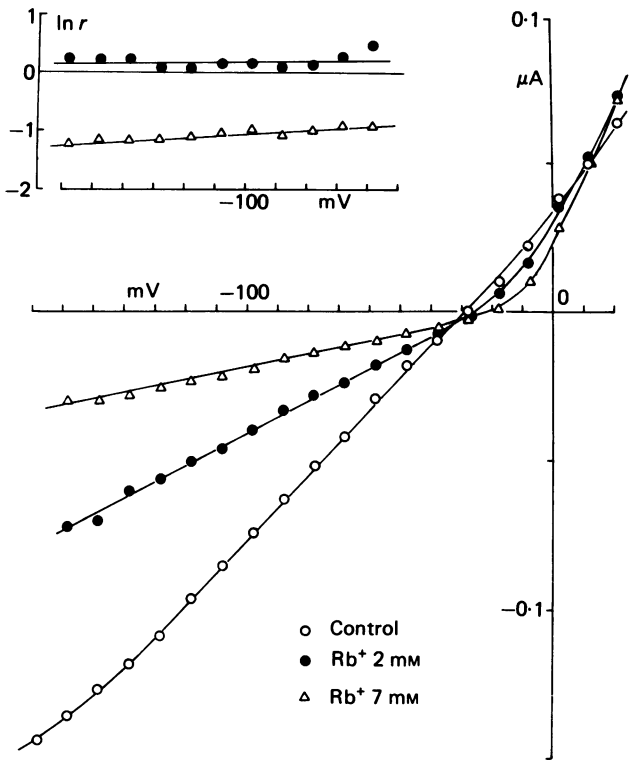

Fig. 10. $i_f(E)$ curves in different Rb^+ concentrations (shown in mM). Control solution contained K^+ 36 mM and Na^+ 35 mM (Tris substitute). Notice lack of voltage-dependence of block, and the presence of cross-over at positive potentials. The inset shows the voltage-dependence of block expressed in terms of relative blocking ratio $r = I_{Rb}/(I - I_{Rb})$. When eqn. (1) is applied to Rb^+ block, values of δ deduced by the slopes of the least-squares fitting lines are 0·02 and 0·09, respectively for upper and lower curve.

Blockade induced by Rb^+ ions

Rubidium ions, like caesium ions, are known to interact with K^+-permeable channels in several tissues (Adrian, 1964; Bezanilla & Armstrong, 1972; Hagiwara & Takahashi, 1974). Fig. 10 shows that the i_f channel also is blocked by Rb^+, although in comparison with Cs^+ higher Rb^+ concentrations are required for a similar blocking effect. From the I–V curves in Fig. 10 the block induced by Rb^+ displays little voltage-dependence, in contrast with that due to Cs^+. Plotting on a semilog scale the relative

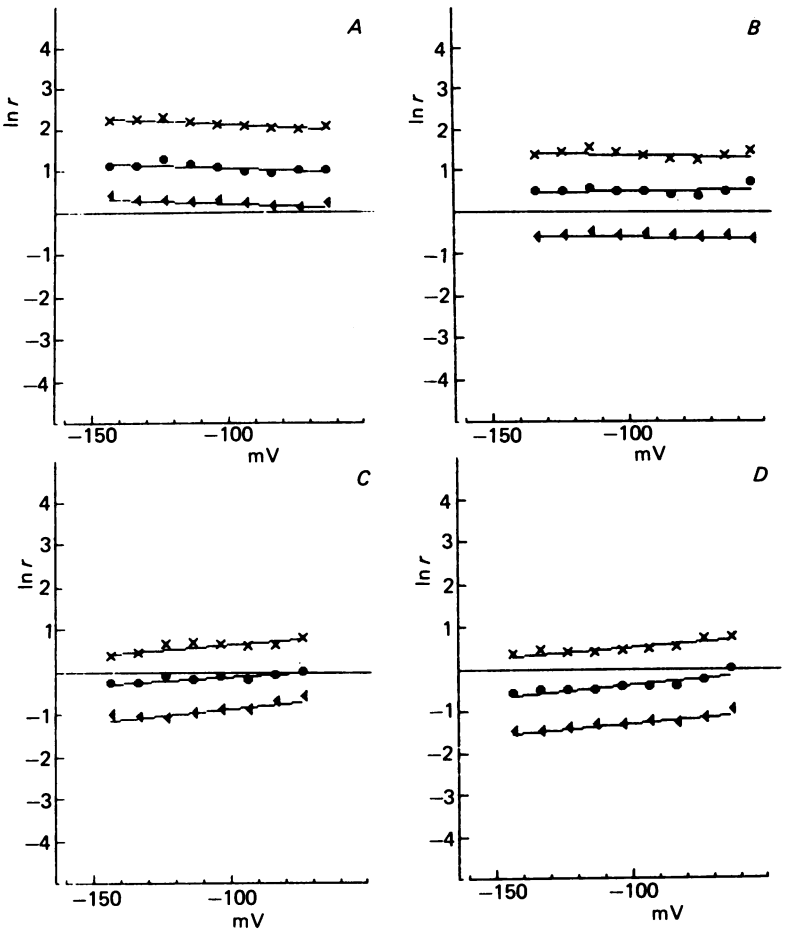

Fig. 11. Voltage-dependence of Rb^+ block. Rb^+ 1 (×), 3 (●) and 10 (◀) mM were added to four different control solutions containing K^+ and Na^+ respectively in the following concentrations (in mM): 6, 70 (*A*), 18, 70 (*B*), 6, 14 (*C*) and 18, 14 (*D*). Na was substituted by Tris. The method for obtaining these plots is identical to that described in Fig. 3. Values of δ calculated from slopes are (top to bottom): −0·085, −0·069, −0·067, (*A*), −0·023, 0·019, −0·016 (*B*), 0·118, 0·086, 0·157 (*C*) and 0·117, 0·140, 0·137 (*D*). Mean δ in this experiment is $0{\cdot}043 \pm 0{\cdot}09$.

blocking ratio $r = I_{Rb}/(I - I_{Rb})$ against membrane potential in the upper part of Fig. 10 produces nearly flat lines for the two Rb^+ concentrations shown. If the same model of channel blockade used for Cs^+ is adopted, these data would indicate that the block induced by Rb^+ occurs at a site near the outer membrane surface.

The voltage-dependence of the Rb^+ block is studied in Fig. 11 for an experiment where Rb^+ in concentrations of 1, 3 and 10 mM was added to solutions containing different K^+ and Na^+ concentrations. As observed with the block induced by Cs^+, changing external K^+ or Na^+ does not appear to have appreciable effects on the value of δ, which is close to zero in all conditions. Fig. 12 shows the concentration-dependence of the Rb^+ block for the same experiment as in Fig. 11. Again, as with

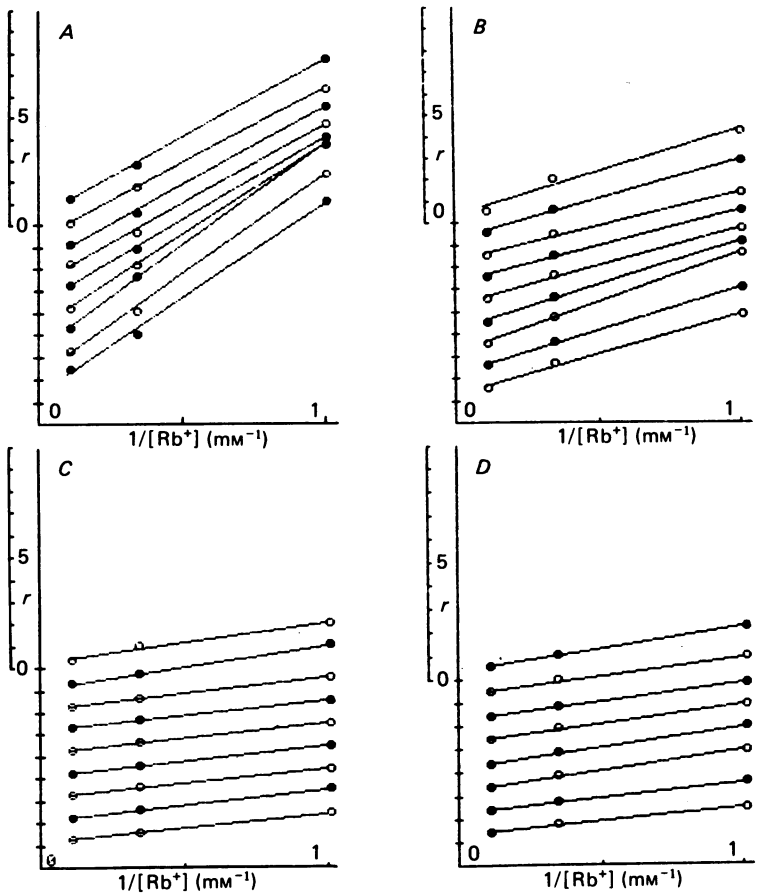

Fig. 12. Concentration-dependence of Rb^+ block for the same experiment shown in Fig. 11. Panels *A–D* correspond to the same reference solutions as in Fig. 11. The explanation of this Figure is analogous to that of Fig. 4. The relative blocking ratio $r = I_{Rb}/(I-I_{Rb})$ is calculated at different potentials for all Rb^+ concentrations used, and plotted against reciprocal of Rb^+ concentration. Top curves correspond to −64 (*A*, *D*), −54 (*B*) and −74 mV (*C*), and lower curves (shifted vertically for clarity) to increasingly more negative potentials (10 mV steps). Notice that apart from some expected scattering, the slope of least-squares fitting lines (representing $k(E)$ in eqn. (6*b*) for Rb^+ block) shows no obvious dependence on membrane potential, but does depend on the ionic conditions.

Cs^+, straight lines can be used to fit the plots of the relative blocking ratio against 1/[Rb] for each membrane potential, indicating that to a first approximation in the far negative voltage range Woodhull's model applies. As expected with a voltage-independent blockade, for each set of ionic conditions the dissociation constant $k(E)$ of the binding reaction of Rb^+ to its blocking site, given by the slope of the least-squares fitting lines in Fig. 12, does not vary with the membrane potential. A decrease in the dissociation constant seems, however, to occur when either the Na^+ concentration is decreased, or the K^+ concentration is raised (compare panel *A* with panels *B* and *C* in Fig. 12). This effect is also evident when plotting in semilog scale

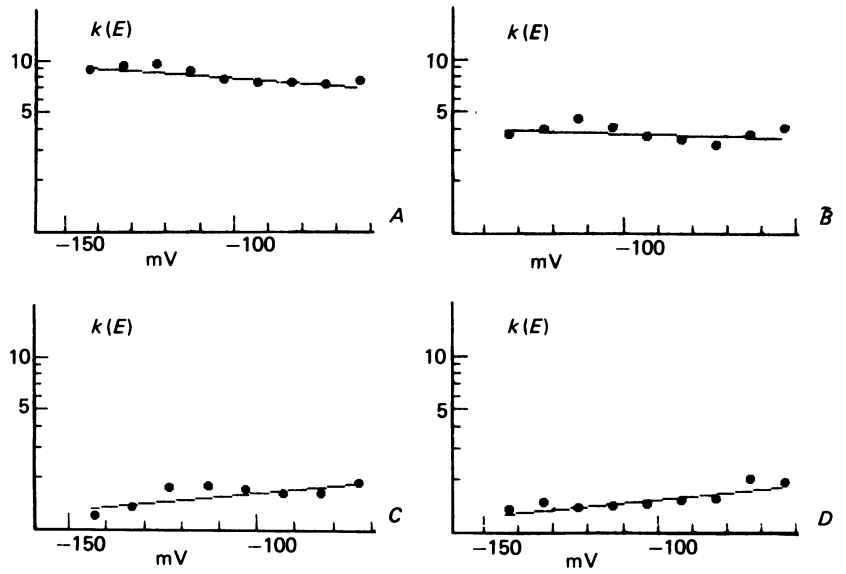

Fig. 13. Voltage-dependence of the dissociation constant $k(E)$ for the Rb^+ blocking reaction, from the same experiment as shown in Figs. 11 and 12. Data points obtained as explained in Fig. 5. Values of the zero-voltage dissociation constant k_0 for Rb^+ binding deduced from these plots are (in mM): 5·4 (*A*), 3·3 (*B*), 2·6 (*C*) and 2·4 (*D*).

TABLE 3. Values of δ and k_0 for Rb^+-induced blockade calculated from six experiments (*a–f*) in various K^+ and Na^+ concentrations

$[Na^+]$ (mM)	$[K^+]$(mM) 6	9	18	24	36
14	*f* 0·121 ± 0·03 (3)		*f* 0·131 ± 0·01 (3)	*c* 0·070 (1)	
				d 0·062 ± 0·03 (3)	
	f 2·57		*f* 2·38	*d* 1·42	
35	*b* 0·277 ± 0·04 (2)	*e* 0·054 ± 0·03 (4)	*a* 0·088 ± 0·04 (2)	*e* 0·040 ± 0·03 (4)	*b* 0·055 ± 0·05 (2)
	e 0·009 ± 0·03 (4)		*b* 0·074 ± 0·004 (2)		
	e 4·71	*e* 2·64	*a* 2·59	*e* 2·06	*b* 2·22
			b 3·27		
70	*f* −0·074 ± 0·01 (3)		*f* −0·007 ± 0·02 (3)	*d* −0·035 ± 0·02 (3)	
	f 5·41		*f* 3·30	*d* 2·13	
140				*d* −0·043 ± 0·05 (3)	
				d 4·74	

The method for obtaining these values and the way they are reported are identical to those used for the Cs^+-induced blockade (see Tables 1 and 2). In each panel upper figures represent values of δ, and lower figures values of k_0.

(Fig. 13) the slopes of the best-fitting lines to the data in Fig. 12 against membrane potential. Following the same procedure used in Fig. 5 above, extrapolation to $E = 0$ mV of these plots yields the values of k_0, the zero-voltage dissociation constant of the Rb^+ binding reaction. From Fig. 13 k_0 is calculated to be 5·41, 3·30, 2·57 and 2·38 mM for the 6 mM-K^+, 70 mM-Na^+ (*A*), 18 mM-K^+, 70 mM-Na^+ (*B*), 6 mM-K^+, 14 mM-Na^+ (*C*) and 18 mM-K^+, 14 mM-Na^+ (*D*) solutions respectively, indicating that in high-K^+, low-Na^+ solutions lower Rb^+ concentrations are required to half-saturate

its channel blocking site. Table 3 summarizes the results from $n = 5$ experiments where Rb^+ was tested in different ionic conditions, and reports values of δ and k_0 calculated as explained above. In all conditions values of δ close to zero are obtained, reinforcing the view that the block occurs at or near the external mouth of the channel. The k_0 reduction in high K^+, low Na^+ solutions is also confirmed. While the

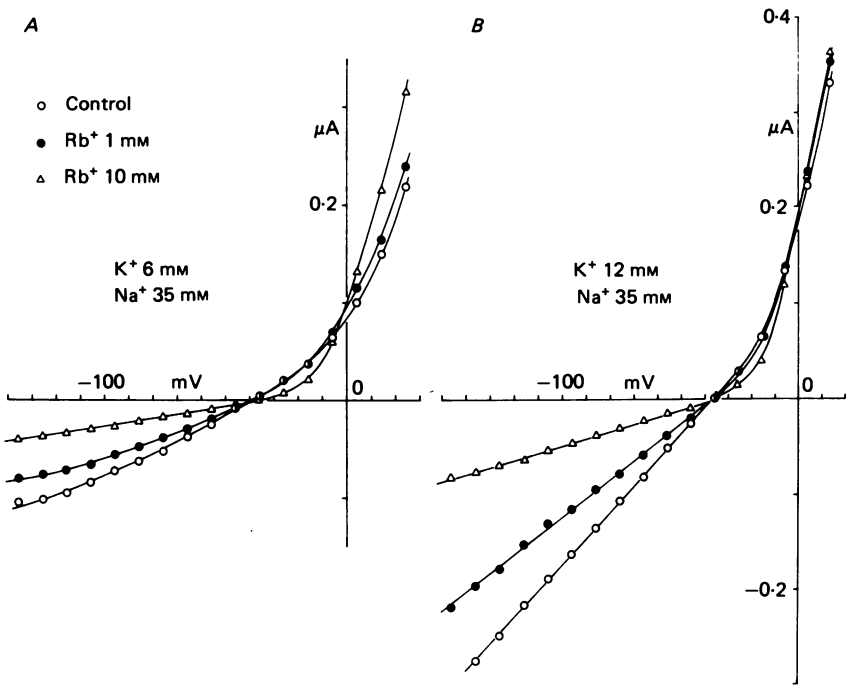

Fig. 14. Activatory effect of Rb^+ 1 and 10 mM in an experiment where the K^+ concentration was changed from 6 to 12 and to 24 mM (curves in 24 mM are not shown). Na^+ concentration was 35 mM throughout (choline substitute). As seen with Cs^+, the current increase in the outward direction caused by Rb^+ is more pronounced in low K^+ concentrations.

effect of Na^+ on k_0 is consistent with competition between Na^+ and Rb^+ ions for the Rb^+-blocking site, the effect of K^+ requires a more complex interaction between K^+ and Rb^+ ions. It is possible that the 'activating' reaction of K^+ ions includes a facilitation of Rb^+ binding, but the present data are not sufficient to verify this possibility.

Activation-like action of Rb^+

The experiment in Fig. 10 shows that, as observed with Cs^+, cross-over of I–V curves is also seen when Rb^+ is added. Thus, Rb^+ too could exert an activating action on the i_f channel. In the experiment shown in Fig. 14 Rb^+ in different concentrations was applied to three solutions containing 6, 12 and 24 mM-K^+ (24 mM-K^+ curves are not shown). The current increase induced by Rb^+ is similar to that seen with Cs^+: it is more pronounced in low-K^+ solutions, in agreement with the view that there is

competition between Rb^+ and K^+ in their activating action. Results similar to those shown in Fig. 14 have been found in two more experiments where Rb^+ was applied to solutions with different K^+ concentrations. The same effect, although less pronounced, has been observed on changing the external Na^+ concentration ($n = 2$). These results agree with the hypothesis that the Rb^+-induced current increase, like that caused by Cs^+, is due to Rb^+ ions binding to the channel 'activating' site.

DISCUSSION

Block of the i_f channel by Cs^+ and Rb^+ ions

Cs^+-induced blockage of K^+-permeable channels has been extensively investigated in skeletal muscle (Gay & Stanfield, 1977), the starfish egg cell (Hagiwara *et al.* 1976), the node of Ranvier (Dubios & Bergman, 1977) and the squid axon (Adelman & French, 1978). In cardiace muscle Cs^+ has been shown to have a blocking action on the pace-maker current in the Purkinje fibre and the SA node (Isenberg, 1976; DiFrancesco & Ojeda, 1980; DiFrancesco, 1981*a*) and to induce a voltage-dependent blockade on the time-independent (i_{K1}) channel in Purkinje fibres (Carmeliet, 1979). The results described here indicate that low concentrations of Cs^+ block the i_f channel in a voltage- and concentration-dependent fashion. In the presence of Cs^+, the i_f current reduction is greater at more negative voltages, as expected for a block produced by the binding of Cs^+ ions to a site within the membrane. Assuming a one-to-one ion-channel ratio, Cs^+ binding can be described by the reaction

$$\mathrm{Cs} + \mathrm{S} \underset{\beta}{\overset{\alpha}{\rightleftharpoons}} \mathrm{CsS}, \tag{3}$$

where S represents the open channel and CsS the channel blocked after Cs^+ binding. If the total current I_{Cs} passing through the channels at a given Cs^+ concentration is made proportional to the fraction of channels in the S state, the steady-state expression relating current and Cs^+ concentration is readily derived from eqn. (3) as

$$r = \frac{\mathrm{I_{Cs}}}{I - I_{Cs}} = \frac{\beta}{\alpha}\frac{1}{[\mathrm{Cs}]}. \tag{4}$$

Following Eyring's rate theory (Glasstone, Laidler & Eyring, 1941) the binding and unbinding reactions are associated with elementary jumps over an energy barrier, which in this case will be located somewhere between the outer membrane surface and the inner binding site. Defining as δ_α (δ_β) the 'electrical' distance between peak of the energy barrier and outer membrane surface (inner binding site), the rate constants α and β of reaction (3) are related to the membrane potential by the exponential functions:

$$\alpha = \alpha_0 \exp\left(-\delta_\alpha \frac{E}{RT/F}\right), \tag{5a}$$

$$\beta = \beta_0 \exp\left(\delta_\beta \frac{E}{RT/F}\right), \tag{5b}$$

which inserted into eqn. (4) give

$$\frac{I_{Cs}}{I-I_{Cs}} = k(E)\frac{1}{[Cs]}, \tag{6a}$$

$$k(E) = k_0 \exp\left(\delta \frac{E}{RT/F}\right), \tag{6b}$$

where $k_0 = \beta_0/\alpha_0$ is the equilibrium constant of reaction (3) at $E = 0$ mV, $\delta = \delta_\alpha + \delta_\beta$ is the 'electrical' distance between blocking site and outer membrane surface, expressed as a fraction of membrane thickness (see Hille, 1975) and R, T and F have their usual meaning. Eqns. (6*a*) and (6*b*) are those used for fitting the data here presented and, at least in a limited range of the far negative region of the $\bar{i}_f(E)$ relation, satisfactorily describe the concentration- and voltage-dependence of the Cs^+-induced blockade of the i_f channel.

The model outlined above is a simpler version of that used by Woodhull (1973) to describe the H^+ block of the Na-channel in the node of Ranvier, and does not account for the possibility that Cs^+ ions can enter the channel from inside the cell. The value of δ obtained by using eqns. (6) for the Cs^+-induced block is $0{\cdot}71 \pm 0{\cdot}13$ ($n = 102$), and does not vary appreciably with either the external Na^+, K^+ or Cs^+ concentrations. This value is far from that of 1·5 obtained by Hagiwara *et al.* (1976) in the starfish egg cell, but is not very different from that of 0·62 found by Dubois & Bergman (1977) for the K-channel in the node of Ranvier. This similarity may, however, be fortuitous, given that this channel is K^+-selective, and therefore its structure may not be comparable to that of the i_f channel. The equilibrium constant k_0 of the Cs^+ blocking reaction, as derived using eqn. (1), is found to range between 0·5 and 3·7 mM (mean k_0 is $2{\cdot}19 \pm 0{\cdot}92$ mM, $n = 16$). The extrapolation method used to measure the dissociation constant at $E = 0$ mV (see Fig. 5) is not precise enough, however, to avoid a relatively large scattering, and possible effects of K^+ and /or Na^+ on Cs^+ binding are better observed at more negative potentials. At $E = -100$ mV the dissociation constant of Cs^+ binding appears to increase with the external Na^+ concentration in some cases (two out of five in Table 2), which would be consistent with a competition between Cs^+ and Na^+ ions for the same site. However, from Table 2 a significant increase in $k(-100)$ is not always observed on raising the Na^+ concentration, and no clear trend is evident on changing external K^+.

The blockade induced by Rb^+ can also be described by the same type of equations as eqns. (6). As for Cs^+, δ does not appear to depend on external Na^+, K^+ or Rb^+ concentrations, and its low mean value of $0{\cdot}05 \pm 0{\cdot}08$ ($n = 42$) suggests that the Rb^+ block occurs at or near the pore entrance. The value of k_0 for the Rb^+-induced blockade is seen to change in different ionic conditions, being lower in low-Na^+, high-K^+ solutions. The accuracy of the extrapolation method used to determine k_0 is obviously higher for lower values of the slopes of the $k(E)$ plots. For this reason the measurement of k_0 for Rb^+ blocking (Fig. 13) can be considered to be more reliable than that for Cs^+ blocking. k_0 measured in 14–140 mM-Na^+ and 6–36 mM-K^+ solutions varies between 1·4 and 5·4 mM, a range similar to that found for the zero-voltage equilibrium constant of Cs^+ binding.

Activating action of K^+ on the i_f channel

The presence of cross-over phenomena and the extent by which the slope of the $\bar{i}_f(E)$ relation increases when the external K^+ concentration is augmented, imply some kind of action of K^+ on the channel conductance. Indeed, these phenomena would be hard to explain by assuming that the only effect of changing external K^+ is to change the current driving force. The data of Figs. 6 and 7 are consistent with the idea that external K^+ ions activate the channel with a one-to-one stoichiometry, according to simple Michaelis–Menten kinetics. A mean value of $44{\cdot}2 \pm 5{\cdot}6$ mM is obtained for the dissociation constant of the K^+ binding to the 'activatory' site.

The measurements here described do not distinguish between a channel all-or-nothing activation process, or a modulation of open channel conductance induced by K^+, even though the evidence that a first-order reaction scheme is able to fully explain the experimental data obviously favours the former interpretation. According to the all-or-nothing hypothesis, K^+-induced activation would be described by a simple one-to-one reaction:

$$K + S \rightleftharpoons KS, \tag{7}$$

where now the complex KS represents a channel in the 'activated' state. The concentration of the complex KS in reaction (7) is proportional to the fraction n of conducting channels. Defining as $\bar{g}_{fM}(E)$ the maximal measurable pace-maker conductance at a given potential E, such that $\bar{g}_f(E) = n \cdot \bar{g}_{fM}(E)$, the equilibrium state of reaction (7) is described by the eqn:

$$\frac{1}{\bar{g}_f(E)} = \frac{1}{n \cdot \bar{g}_{fM}(E)} = \frac{1}{\bar{g}_{fM}(E)} + \frac{k_K}{\bar{g}_{fM}(E)} \cdot \frac{1}{[K]}, \tag{8}$$

k_K being the equilibrium constant of (7). Eqn. (8) is that used to analyse the data shown in Fig. 7. If, therefore, the activatory action or K^+ ions consists of a channel opening process, raising the external K^+ concentration would simply result in an increased number of operating channels (that is, channels able to conduct when activated by hyperpolarizations). Thus, the measured $\bar{i}_f(E)$ relation should correspond to the product of the single-channel I–V characteristic (at the proper K^+ concentration) and the number of operating channels. This also implies that the method of selecting in each experiment a voltage range for least-squares fitting of $\bar{i}_f(E)$ relations in different K^+ concentrations does not necessarily require that the I–V curves in that range are linear. In fact, even with non-linear relations, the method is equivalent to averaging the fully activated slope conductance in the selected region, and the ratio between two mean values in two different K^+ concentrations thus coincides with the ratio between fractions of K^+-activated channels.

A K^+ channel activation has also been proposed for the K-channel in the frog node of Ranvier (Dubois & Bergman, 1977) and for the inward-rectifying K-channel in skeletal muscle (Standen & Stanfield, 1978*b*). It is interesting to observe that, as mentioned above, these channels are also blocked by Cs^+ in a voltage-dependent fashion. These similarities argue in favour of the view that, within certain limits, part of the structural properties of different channels might to some extent be comparable.

It is, however, important to add that, until more suitable experimental information

is available to clarify the problem of how the K^+-induced current increase occurs (by, for example, noise measurements, Stevens, 1972), the proposed activation mechanism can only be regarded as a useful description of experimental results.

Interaction between K^+, Cs^+ and Rb^+ in their activating action

If external K^+ interacts with a channel site to produce the observed current increase, binding of other ions to the same site could, in competition with K^+, give rise to a similar effect. This assumption readily explains why Cs^+ and Rb^+ produce, in spite of their blocking effect which becomes progressively more evident at more negative potentials, cross-over of I–V curves in solutions where they are present in different concentrations (Figs. 2, 9, 10 and 14), and how the cross-over depends on external K^+ activity (Figs. 9 and 14).

Unlike that due to K^+, however, this action of Cs^+ and Rb^+ cannot be studied properly, as it cannot be separated from the blocking effect of the same ions, and the voltage range where it appears is near the resolution limit of the present experiments. Qualitative evidence like that shown in Figs. 9 and 14 is nevertheless sufficient to verify that the Cs^+- and Rb^+-induced current increase in the positive voltage range of the $\bar{i}_f(E)$ relation is inhibited by the presence of K^+, as expected for a competitive interaction with these ions. Although with a lower efficiency than external K^+, external Na^+ is also found to have a competitive action on Cs^+ and Rb^+ binding to the 'activatory' site. This would thus imply a competition between Na^+ and K^+, too. The fact that no such competition is apparent from the k_K data in Fig. 7 can be attributed to a relatively high dissociation constant of Na^+ binding, giving rise to an effect on k_K smaller than data scattering.

It is worth noting that in the frog nerve, together with a voltage-dependent channel blockade, French & Adelman (1976) also found a current increase at positive potentials in Cs^+-containing solutions, which they first attributed to a proper activatory effect of Cs^+, and later to an indirect depressing effect of the high Tris concentrations used in the control solutions before substituting CsCl (Adelman & French, 1978). In the present experiments on i_f such a depressing effect can be excluded, because high Tris HCl solutions are not used, and the activating effect of Cs^+ is present even at low Cs^+ concentrations, and when both in the control solution and in the Cs^+-containing solution choline rather than Tris is used as a substitute for Na^+. The activatory effect of Cs^+ on i_f can also provide an alternative mechanism to explain the increase in steady-state current observed by Isenberg (1976) in sheep Purkinje fibres exposed to high Cs^+ concentrations, and interpreted as due to activation of the Na–K pump by Cs^+.

I am indebted to H. F. Brown and D. Noble for carefully revising and commenting on the manuscript, and to A. Ferroni for encouragement during this work. I should also like to thank D. Janigro for contributing to part of the experiments, and C. Ojeda for help in printing some of the pictures.

REFERENCES

ADELMAN, W. J. & FRENCH, R. J. (1978). Blocking of the squid axon potassium channel by external caesium ions. *J. Physiol.* **276**, 13–25.

ADRIAN, R. H. (1964). The rubidium and potassium permeability of frog muscle membrane. *J. Physiol.* **175**, 134–159.

ARMSTRONG, C. M. (1969). Inactivation of the potassium conductance and related phenomena caused by quaternary ammonium ion injection in squid axons. *J. gen. Physiol.* **54**, 553–575.

BEZANILLA, F. & ARMSTRONG, C. M. (1972). Negative conductance caused by entry of sodium and cesium ions into the potassium channels of squid axons. *J. gen. Physiol.* **60**, 588–608.

BROWN, H. F., DIFRANCESCO, D., KIMURA, J. & NOBLE, S. (1981). Caesium: a useful tool for investigating sino-atrial (SA) node pace-making. *J. Physiol.* **317**, 54*P*.

CARMELIET, E. (1979). Voltage dependent block of inward going rectification in cardiac Purkinje fibres by external Cs ions. *Archs int. Pharmacodyn. Thér.* **242**, 294–295.

CIANI, S., KRASNE, S. & HAGIWARA, S. (1980). A model for the effects of potential and external K^+ concentration on the Cs^+ blocking of inward rectification. *Biophys. J.* **30**, 199–204.

CORONADO, R. & MILLER, C. (1979). Voltage-dependent Cs^+ block of a K^+ channel from sarcoplasmic reticulum. *Nature, Lond.* **280**, 807–810.

DIFRANCESCO, D. (1981*a*). A new interpretation of the pace-maker current in calf Purkinje fibres. *J. Physiol.* **314**, 359–376.

DIFRANCESCO, D. (1981*b*). A study of the ionic nature of the pace-maker current in calf Purkinje fibres. *J. Physiol.* **314**, 377–393.

DIFRANCESCO, D. (1981*c*). Voltage dependence of Cs effects on the pace-maker current in Purkinje fibres. *J. Physiol.* **320**, 31–32*P*.

DIFRANCESCO, D. & OJEDA, C. (1980). Properties of the current i_f in the sinoatrial node of the rabbit compared with those of the current i_{K2} in Purkinje fibres. *J. Physiol.* **308**, 353–367.

DUBOIS, J. M. & BERGMAN, C. (1977). The steady-state potassium conductance of the Ranvier node at various external K-concentrations. *Pflügers Arch.* **370**, 185–194.

FRENCH, R. J. & ADELMAN, W. J. (1976). A capricious blocking ion: cesium can increase potassium channel currents. *Biophys. J.* **16**, 189*a*.

GAY, L. & STANFIELD, P. R. (1977). Cs^+ causes a voltage-dependent block of inward K^+ currents in resting skeletal muscle fibres. *Nature, Lond.* **267**, 169–170.

GLASSTONE, S., LAIDLER, K. J. & EYRING, H. (1941). *The Theory of Rate Processes.* New York: McGraw-Hill.

HAGIWARA, S., MIYAZAKI, S., MOODY, W. & PATLAK, J. (1978). Blocking effects of barium and hydrogen ions on the potassium current during anomalous rectification in the starfish egg. *J. Physiol.* **279**, 167–185.

HAGIWARA, S., MIYAZAKI, S. & ROSENTHAL, N. P. (1976). Potassium current and the effect of cesium on this current during anomalous rectification of the egg cell membrane of a starfish. *J. gen. Physiol.* **67**, 621–638.

HAGIWARA, S. & TAKAHASHI, K. (1974). The anomalous rectification and cation selectivity of the membrane of a starfish egg cell. *J. Membrane Biol.* **18**, 61–80.

HILLE, B. (1975). Ionic selectivity of Na and K channels of nerve membranes. In *Membranes: a series of advances*, Vol. 3, ed. EISENMAN, G., pp. 255–323. New York: Dekker.

HILLE, B. & SCHWARZ, W. (1978). Potassium channels as multi-ion single-file pores. *J. gen. Physiol.* **72**, 409–442.

ISENBERG, G. (1976). Cardiac Purkinje fibres: cesium as a tool to block inward rectifying potassium currents. *Pflügers Arch.* **365**, 99–106.

SANDBLOM, J., EISENMAN, G. & NEHER, E. (1977). Ionic selectivity, saturation and block in Gramicidin A channels. *J. Membrane Biol.* **31**, 383–417.

SIEGELBAUM, S. A. & TSIEN, R. W. (1980). Calcium-activated transient outward current in calf cardiac Purkinje fibres. *J. Physiol.* **299**, 485–506.

SPERELAKIS, N., SCHNEIDER, M. & HARRIS, E. J. (1967). Decreased K conductance produced by Ba^{2+} in frog sartorius fibres. *J. gen. Physiol.* **50**, 1565–1583.

STANDEN, N. B. & STANFIELD, P. R. (1978*a*). A potential- and time-dependent blockade of inward rectification in frog skeletal muscle fibres by barium and strontium ions. *J. Physiol.* **280**, 169–191.

STANDEN, N. B. & STANFIELD, P. R. (1978*b*). Inward rectification in skeletal muscle: a blocking particle model. *Pflügers Arch.* **378**, 173–176.

STEVENS, C. F. (1972). Inferences about membrane properties from electrical noise measurements. *Biophys. J.* **12**, 1028–1047.

WOODHULL, A. M. (1973). Ionic blockage of sodium channels in nerve, *J. gen. Physiol.* **61**, 687–708.